Precision instrument for characterizing shape memory alloy wires in bias spring actuation

Sumanth Chikkamaranahalli, R. Ryan Vallance,[a] and Afzal Khan
Mechanical and Aerospace Engineering Department, The George Washington University, 738 Phillips Hall, 801 22nd Street N.W., Washington, DC, 20052

Eric R. Marsh
Mechanical Engineering Department, The Pennsylvania State University, 21 Reber Building, University Park, Pennsylvania 16802

Osamah A. Rawashdeh, J. E. Lumpp, and Bruce L. Walcott
Electrical and Computer Engineering Department, University of Kentucky, 569 Anderson Hall, Lexington, Kentucky 40506

(Received 4 January 2005; accepted 26 March 2005; published online 20 May 2005)

Some metallic alloys such as Nitinol (NiTi) exhibit the shape memory effect, which is suitable for generating force and displacement when the alloy changes phase during a heating and cooling cycle. These shape memory alloys are often formed into one-dimensional wires, tubes, and ribbons that are preloaded by bias springs to create inexpensive actuators for electromechanical devices. This article describes a new instrument for measuring the quasistatic characteristics of the alloy and the transient performance of bias-spring actuators when resistively heated and convectively cooled. The instrument achieves more accurate measurements by eliminating rolling friction and by sensing force and displacement in line with the bias spring and shape memory alloy wire. Data from the instrument enables calculation of stress and strain at constant temperatures and during actuation cycles. © *2005 American Institute of Physics.* [DOI: 10.1063/1.1920629]

I. INTRODUCTION

Shape memory alloys (SMAs) are formulated to exhibit phase transformations between martensite and austenite at specific temperatures or levels of stress. Without stress, alloys begin a temperature-induced (reverse) transformation from martensite to austenite at the austenite start temperature A_s and finish at the austenite finish temperature A_f. The (forward) transformation from austenite to martensite begins at the martensite start temperature M_s and finishes at the martensite finish temperature M_f. The phase transformation temperatures change when stress is applied to the alloy, and transformations can even be induced at constant temperature with sufficient stress.[1] The martensite fraction ξ, which ranges between zero and one, indicates the progress of the transformation from austenite such that $\xi=0$ when the alloy is completely austenite and $\xi=1$ when the alloy is completely martensite. Stress and strain are produced when these alloys transition phases due to changes in the arrangement of the alloy's crystal lattice. This reversible phenomenon is often called the shape memory effect because reversing the transformation restores the alloy's original shape.

SMAs are often manufactured in one-dimensional shapes like wires, ribbons, and tubes. They are available in various alloy formulations, but one of the most common is Nitinol (55% Ni by weight and 45% Ti by weight). Table I lists the approximate transition temperatures and other relevant properties for the martensite and austenite phases of commercially available Flexinol™ (70 °C) (Dynalloy Inc., Costa Mesa, CA), which produces up to 6% strain and 180 MPa stress during its martensite to austenite transition.[2]

The thermal energy necessary for transition from martensite to austenite is often applied by flowing current through the SMA wire. This enables inexpensive mechanical actuation with electronic control. For example, linear actuators are made by preloading SMA wires with bias springs, as described by Liang and Rogers.[3] SMA wires in similar actuators were recently proposed for vibration control,[4] micro robotics,[5] adaptive airfoils,[6] biomedical devices,[7,8] and many other applications.

Liang and Rogers[9] described a model for predicting the actuation stress and strain produced by an SMA wire when the material properties of the SMA, length of the SMA wire L, cross-sectional area of the SMA wire s, and stiffness of the bias spring k are known. Their model estimates the martensite fraction ξ during the transformation from martensite to austenite with Eq. (1) and during the reverse transformation from austenite to martensite with Eq. (2). The transformation depends on the temperature differences $(T-M_f)$ and $(T-A_s)$ as well as the stress within the wire. The initial martensite fractions, ξ_A and ξ_M, and the four material properties a_M, a_A, b_M, and b_A must also be known. Another approach presented by Brinson[10] separates ξ into stress-induced and temperature-induced martensite fraction.

$$\xi = \frac{\xi_M}{2}\{\cos[a_A(T-A_s)+b_A\sigma]+1\}, \quad (1)$$

[a]Author to whom correspondence should be addressed; electronic mail: vallance@gwu.edu

TABLE I. Material properties for Flexinol™.

Property		Value
Austenite start temperature	A_s	67 °C
Austenite finish temperature	A_f	75 °C
Martensite start temperature	M_s	48 °C
Martensite finish temperature	M_f	38 °C
Modulus of elasticity		
Martensite	E_m	~28 GPa
Austenite	E_a	~83 GPa
Coefficient of thermal expansion		
Martensite	α_m	6.6×10^{-6} 1/°C
Austenite	α_a	11.0×10^{-6} 1/°C
Heat of transformation	H	2.42×10^{3} J/kg

$$\xi = \frac{1-\xi_A}{2}\left\{\cos[a_M(T-M_f)+b_M\sigma]+\frac{1+\xi_A}{2}\right\}. \tag{2}$$

In the work of Liang and Rogers,[3,9] the stress σ produced when the SMA wire transitions from martensite to austenite is approximated with a piecewise continuous function, which is given in Eq. (3). The stress depends upon the prestress σ_o, transient temperature differences, the martensite fraction ξ, and two coefficients, which are the modified thermoelastic modulus Θ' and the modified transformation coefficient Ω'. When the alloy is 100% martensite ($T<A_s$) and 100% austenite ($T>A_f$), the segments are nearly linear with temperature change, and their slopes are significantly less than that during the transformation segment when ($A_s<T<A_f$)

$$\sigma = \begin{cases} \Theta'(T-T_M)+\sigma_o & \text{for } T\leqslant A_s^m \\ \Theta'(T-A_s^m)+\Omega'(\xi-\xi_o)+\sigma_{As} & \text{for } A_s^m\leqslant T\leqslant A_f^m \\ \Theta'(T-A_f^m)+\sigma_{Af} & \text{for } A_f^m\leqslant T \end{cases}. \tag{3}$$

Similarly, the piecewise continuous function given in Eq. (4) models the stress during the transformation from austenite to martensite with two linear segments and a transformation segment

$$\sigma = \begin{cases} \Theta'(T-T_c)+\sigma_c & \text{for } M_s^m\leqslant T\leqslant T_c \\ \Theta'(T-M_s^m)+\Omega'(\xi-\xi_c)+\sigma_{Ms} & \text{for } M_f^m\leqslant T\leqslant M_s^m \\ \Theta'(T-M_f^m)+\sigma_{mf} & \text{for } T\leqslant M_f^m \end{cases}. \tag{4}$$

The strain within the wire as a result of the stress and force applied to the bias spring is computed knowing the spring stiffness k and the length of the SMA wire L with Eq. (5)

$$\varepsilon = \varepsilon_o + \frac{s}{kL}(\sigma+\sigma_o). \tag{5}$$

Based on Eqs. (3)–(5), the response of a bias spring actuator depends upon the temperature changes during heating and cooling, the martensite fraction ξ from Eqs. (1) and (2), several material properties (a_M, a_A, b_M, b_A, Θ', and Ω'), the length of wire L, and the spring rate k. Furthermore, the transient temperature depends upon the current, wire resistance, the heat lost by conduction at the ends of the wire, and the heat lost by convection to ambient air. There is significant uncertainty in several of these factors that are necessary for accurately modeling bias spring actuators with analytical models such as Liang and Roger's. Furthermore, the model of Liang and Rogers is only an approximate solution since it does not accurately model the regions when the transformations start and end (as supported by our experimental data).

The mechanical, thermal, and electrical properties necessary for modeling shape memory alloys during phase transformations vary dramatically with temperature changes or applied stress. The transformation temperatures are frequently determined for unstressed specimens with either differential scanning calorimetry (DSC) or electrical resistivity.[11,12] However, applying stress to the specimen increases the transformation temperatures. Therefore, others conducted conventional tensile tests that gradually increase the stress isothermally and then repeat the experiment at different temperatures.[13,14] Another technique suspends weights from the specimen during cyclic heating, and the transformation temperatures are inferred from plots of strain versus temperature.

A number of instruments were designed and employed to study the response of SMAs under operating conditions found in actuation and control applications. Clingman *et al.*[15] described a tension test apparatus with a pivoting lever arm carrying weights and a thermoelectric module for heating the specimen. They reported issues with lowering the temperature during cooling, friction within the bearings, and maintaining constant temperature along the length of the sample. Others such as Abel *et al.*[11] and Benzaoui *et al.*[16] used a suspended mass to tension the SMA specimen. Song *et al.*[17] used a bias spring to stress the specimen in another instrument that cycled the temperature by resistive heating. Their instrument used a conventional linear bearing that exhibited nonlinear stick–slip friction, and it also did not measure force during the actuation cycle. Ma and Song[18] described a similar instrument that used bias spring preloading without force measurement, and this instrument also contained a linear bearing and pulleys that caused rolling friction.

A precision instrument was developed to accurately characterize the SMA wire under its intended operating conditions with bias spring preloading and resistive heating. This paper describes the instrument, improvements over our previous instrument described by Chikkamaranahalli *et al.*,[19] and demonstrates quasistatic measurements. These design improvements are based on the design principles of precision machines and instruments.[20,21] Other details regarding the mechanical design of the instrument are available from Chikkamaranahalli *et al.*[22] The instrument measures force and displacement within a specimen over many excitation cycles and many hours for static, quasistatic, and transient temperatures. Other measured parameters include the temperature of the SMA element, the stiffness of the bias spring, and the current flowing through the wire. The transient excitation current is programmable with a microcontroller that is interfaced to the instrument's PC-based data acquisition system.

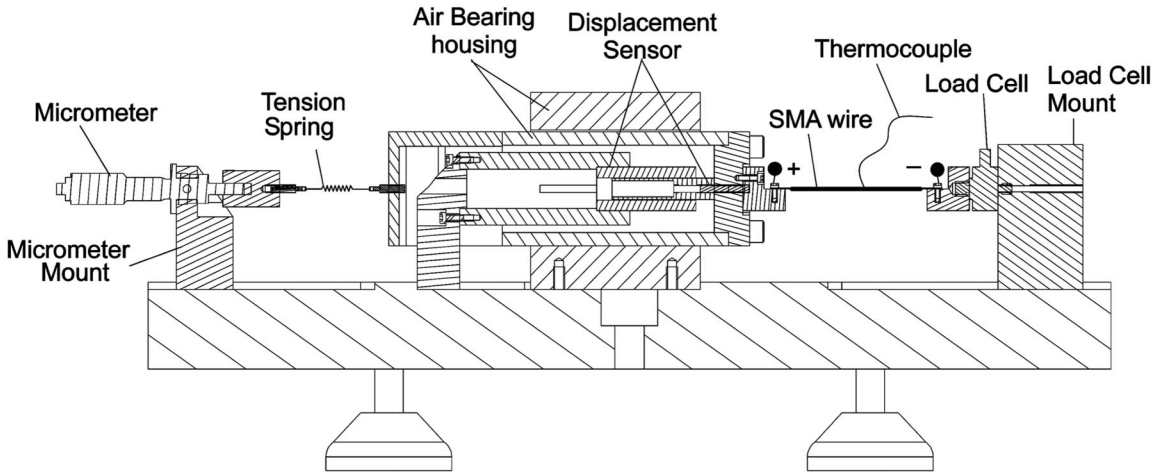

FIG. 1. Schematic of the instrument for characterizing SMA in bias spring actuation.

II. DESIGN OF THE INSTRUMENT

The instrument is schematically illustrated in Fig. 1. The SMA specimen is suspended between a resistive load cell and an externally pressurized air bearing (New Way, S40400305). The air bearing provides translation without static friction, and the dynamic friction due to viscous effects in the air film is negligible for quasistatic measurements. A tension spring is suspended between the air bearing and a non-rotating spindle micrometer (Starrett, 261L) with 12.7 mm travel. The tension spring, SMA specimen, load cell, and displacement sensor are colinear to improve the accuracy of displacement measurements. If the SMA specimen does not pull through the bearing's center of stiffness, then it produces angular error motion (due to bearing pitch compliance and elastic deformation within the instrument), and the magnitude of this error motion increases proportionally to the force in the SMA specimen. If the displacement sensor is offset (not colinear) with the SMA specimen, then these angular errors will affect the accuracy of the displacement measurements in accordance with Abbe's principle.[21,23] Extending or retracting the micrometer adjusts the preload force and stress within the SMA specimen prior to actuation, and the load cell measures the magnitude of the preload. Adjusting the position of the mounts for the load cell or micrometer accommodates various lengths of SMA specimens and tension springs.

The force generated when the SMA specimen transforms between phases is measured with a high-sensitivity load cell (Honeywell Sensotec, Model 31), having a resolution of 0.5 mN over a range of 9.8 N. The translation of the air bearing is measured with a frictionless, noncontact analog displacement sensor (Sentech, DCFS 3/4) capable of measuring displacements up to 19 mm. The temperature of the SMA specimen is measured with a fine-gauge T-type thermocouple and an amplifier (Omega, Model SMCJ-T) that is joined to the SMA specimen with electrically insulating but thermally conductive paste (Omegatherm 201). The electric current through the specimen is measured with a noncontact sensor (F.W. Bell Technologies, mA-2000) that is sensitive up to 2 A with a resolution of 0.1 mA.

The signal transmission between the controller, data acquisition system, and instrument are illustrated in Fig. 2. A host PC runs a user interface and contains a PCI data acquisition card (IoTech, DAQBoard 2001) with a four channel analog simultaneous sample and hold card. Test parameters such as the quantity of actuation cycles, current profile, current duration, and cooling time are entered into the user interface, which communicates via RS232 with the experiment controller that regulates transient experiments. A trigger from

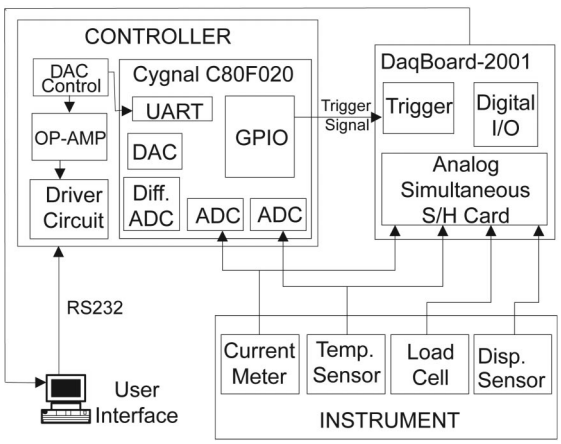

FIG. 2. Data acquisition system and controller.

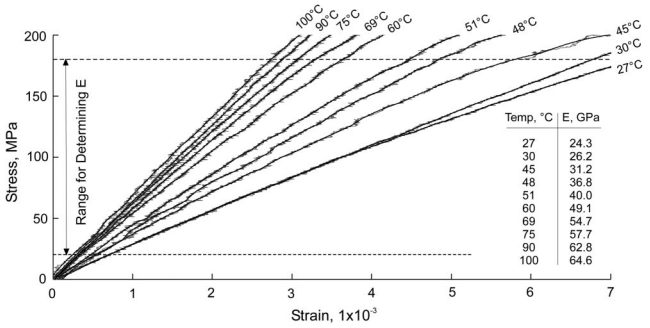

FIG. 3. Stress–strain curves for ten temperatures between 27 and 100 °C. The specimen's modulus of elasticity was determined as the slope of the filtered curves between 20 and 180 MPa.

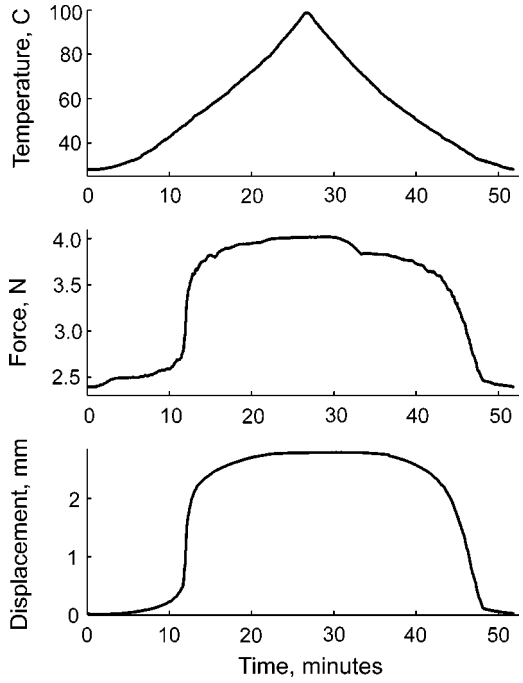

FIG. 4. Time history of current, force, and displacement during a quasistatic measurement, sampled at 10 Hz and low-pass filtered at 0.2 Hz.

the microcontroller's general-purpose input/output pin initiates simultaneous data sampling of current, temperature, force, and displacement. A metal–oxide–semiconductor field effect transistor switching transistor regulated at its gate by an amplified analog signal from the microcontroller's digital to analog converter modulates the current profile as a function of time.

III. RESULTS AND DISCUSSION

Stress as a function of strain at various specimen temperatures is calculated from the force and displacement data. This enables the specimen's modulus of elasticity to be determined as a function of temperature. The temperature of the specimen is set by flowing constant current through the specimen until it reaches a steady temperature as indicated by the thermocouple. Adjusting the micrometer increases the stress within the wire, and measurements from the force and displacement sensors are recorded by the DAQ system. The displacement sensor directly measures the elongation of the SMA specimen, which is significantly less than the elongation of the spring. The engineering stress and strain are calculated by dividing the measured force by the specimen cross-sectional area and length, respectively.

Figure 3 illustrates typical measurements for a Flexinol™ specimen with dimensions of $\varnothing 0.152 \times 50.8$ mm, measured for temperatures ranging between room temperature and 100 °C. The measured data are plotted in gray and data filtered with a 0.1 Hz low-pass filter is shown in black. For each curve, a value for the specimen's modulus of elasticity E (slope of stress–strain curve) is determined using data within the 20–180 MPa range. The table included within the figure gives the dependence of the specimen's modulus of elasticity on temperature, which ranges from about 24 GPa, at room temperature, to about 65 GPa at

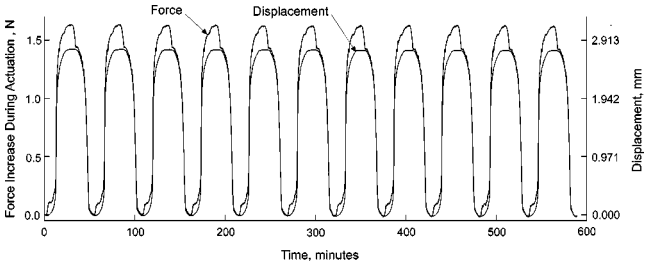

FIG. 5. Measured displacement and force for 11 quasistatic actuation cycles over nearly 600 min, sampled at 10 Hz and low-pass filtered at 0.2 Hz.

100 °C. Troisfontaine *et al.*[24] reported similar values of 25 and 70 GPa for Flexinol-HT in the low and high temperature phases. Some softening of the specimen is indicated by the reduction in slope of the stress–strain curves at lower temperatures, but the softening is not evident at higher temperatures associated with the austenite phase. Similar softening is observed in the data of Troisfontaine *et al.*[24] and Miller and Lagoudas[13] who presented stress–strain diagrams for NiTi and NiTiCu wires. Despite softening, it is still common to report the linearized modulus for engineering analyses.

Figure 4 shows data recorded during the quasistatic actuation of a Flexinol™ specimen with dimensions of $\varnothing 0.152 \times 50.8$ mm. The measured data were low-pass filtered in the frequency domain using a sharp cutoff at 0.2 Hz. During these measurements, the current was increased to 520 mA, held steady for 30 s, and decreased to 0 mA using increments and decrements of 0.1 mA with each step lasting 3 s. Before flowing current, the specimen was preloaded to 2.4 N, which corresponds to a stress of around 130 MPa. During heating, the temperature increased from 27 to 97 °C, which caused the stress in the specimen to increase to 221 MPa while the specimen shortened by 2.781 mm.

To demonstrate the instrument's repeatability and long-term stability, the specimen was cycled eleven times through the same current profile, lasting nearly 600 min. During these 11 cycles, the bias spring returned the specimen to its original length within about 2 μm, which is only 0.07% of the specimen's contraction. Figure 5 shows the recorded history of the measured displacements and force. The scale of the displacement ordinate is determined as the force ordinate

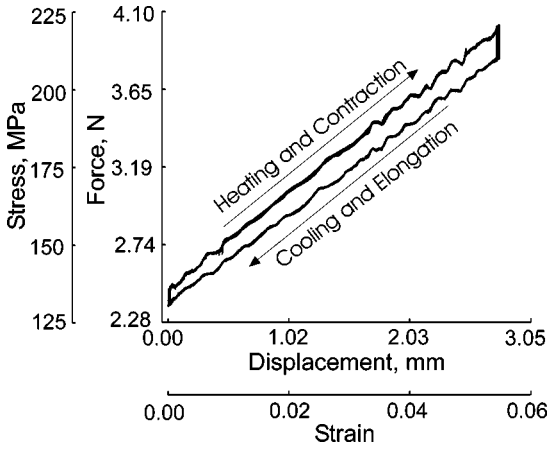

FIG. 6. Stress and force as a function of strain or displacement eleven quasistatic actuation cycles, from the time history data shown in Fig. 5.

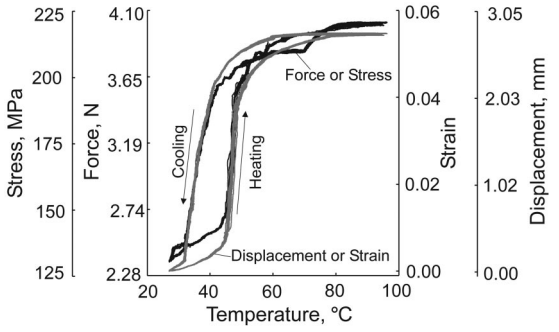

FIG. 7. Stress (or force) and strain (or displacement) as functions of SMA temperature for 11 repeated actuation cycles.

divided by the calibrated stiffness of the bias spring. This illustrates the agreement between the measured force and the force within the bias spring during the cooling of the SMA specimen. However, the forces do not match during the heating cycle; it is especially evident at the starting and ending of the heating periods.

During a single actuation cycle, the SMA specimen does work in translating the mass and stores potential energy within the bias spring. The potential energy stored within the spring is then expended in stretching the SMA specimen back to its original length. Data from time history enables this cycle to be quantified graphically by plotting the measured force as a function of displacement. This yields a loop in which the upper curve corresponds with heating and contraction while the lower curve corresponds with cooling and relaxation. Figure 6 shows these cycles for the 11 quasistatic cycles shown in Fig. 5. The repeatability of the recorded data is extraordinary, typically less than 2 μm, for the entire eleven cycles over nearly 600 min. At this time, we are uncertain whether the ripples in these loops are the result of the instrument or the SMA transformation. However, they are repeatable and appear to flip sign with the direction of motion.

Figure 7 shows the change in stress (or force) and strain (or displacement) as a function of the temperature of the SMA specimen for the eleven quasistatic cycles. Little discernable difference is evident from the loop for each cycle. Rapid changes in the measured force and displacement should occur in the vicinity of the phase transformation temperatures. However, the experimentally observed transformation temperatures do not match the manufacturer's specifications given in Table I. This is not surprising since the transformation temperatures of Nitinol wires under stress differ from those measured by DSC.[11] It is also interesting that linear dependence for the stress above A_f and below M_f, which are predicted by the model of Liang and Rogers given in Eqs. (3) and (4), are not distinct. The strain reached a steady limit just under 6%.

This article describes an instrument for precisely characterizing SMA specimens used as electromechanical actuators by resistive heating. The instrument attains high measurement accuracy by eliminating bearing friction and by arranging the SMA specimen, spring, force sensor, and displacement sensor in a common line to eliminate Abbe offset. An experiment controller enables the current profile to be adjusted for a wide range of quasistatic and transient heating. Measurements of 11 quasistatic cycles of the SMA specimen over nearly 600 min demonstrate the repeatability and long-term stability of the instrument. Measured data is used to observe the work performed by the specimen and the stress/strain that is generated, as a function of temperature. In addition, the instrument can also be used to observe the modulus of elasticity as a function of temperature.

ACKNOWLEDGMENTS

The authors gratefully acknowledge Intranasal Technology, Inc. (Lexington, KY) for their financial support and Honeywell Sensotec (Columbus, OH) for donating a load cell and its amplifier.

[1] L. Delaey, R. V. Krishnan, H. Tas, and H. Warlimont, J. Mater. Sci. **9**, 1536 (1974).
[2] Dynalloy Inc. Costa Mesa, CA 92626-3405.
[3] C. Liang and C. A. Rogers, ASME J. Mech. Des. **114**, 223 (1992).
[4] S. Saadat, J. Salichs, M. Noori, Z. Hou, H. Davoodi, I. Bar-on, Y. Suzuki, and A. Masuda, Smart Mater. Struct. **11**, 218 (2002).
[5] Q. Chang-jun, M. Pei-sun, and Y. Qin, Sens. Actuators, A **113**, 94 (2004).
[6] J. K. Strelec, D. C. Lagoudas, M. A. Khan, and J. Yen, J. Intell. Mater. Syst. Struct. **14**, 257 (2003).
[7] T. Duerig, A. Pelton, and D. Stockel, Mater. Sci. Eng., A **273**, 149 (1999).
[8] A. L. McKelvey and R. O. Ritchie, J. Biomed. Mater. Res. **47**, 301 (1999).
[9] C. Liang and C. A. Rogers, J. Intell. Mater. Syst. Struct. **8**, 285 (1997).
[10] L. C. Brinson, J. Intell. Mater. Syst. Struct. **4**, 229 (1993).
[11] E. Abel, H. Luo, M. Pridham, and A. Slade, Smart Mater. Struct. **13**, 1110 (2004).
[12] J. Uchil, Pramana, J. Phys. **58** 229-242 (2002).
[13] H. Tobushi, S. Yamada, T. Hachisuka, A. Ikai, and K. Tanaka, Smart Mater. Struct. **5**, 788 (1996).
[14] D. A. Miller and D. C. Lagoudas, Smart Mater. Struct. **9**, 640 (2000).
[15] D. J. Clingman, F. T. Calkins, and J. P. Smith, Proc. SPIE **5053**, 219-229 (2003).
[16] H. Benzaoui, C. Lexcellent, N. Chaillet, B. Lang, and A. Bourjault, J. Intell. Mater. Syst. Struct. **8**, 619 (1997).
[17] G. Song, V. Chaudhry, and C. Batur, Smart Mater. Struct. **12**, 223 (2003).
[18] N. Ma and G. Song, Smart Mater. Struct. **12**, 712 (2003).
[19] S. B. Chikkamaranahalli, R. R. Vallance, O. A. Rawashdeh, J. E. Lumpp, and B. L. Walcott, Proceedings of the International Conference on Shape Memory and Super Elastic Technologies (SMST). Pacific Grove, CA., May 4–8, 2003, pp. 583–593.
[20] A. Slocum, *Precision Machine Design* (Society of Manufacturing Engineers, Dearborn, MI, 1992).
[21] P. Schellekens, N. Rosielle, H. Vermeulen, M. Vermeulen, S. Wetzels, and W. Pril, CIRP Ann. **47**, 557 (1998).
[22] S. B. Chikkamaranahalli, R. R. Vallance, O. A. Rawashdeh, J. E. Lumpp, and B. Walcott, Proceedings of the 17th Annual Meeting of the American Society for Precision Engineering. St. Louis, MO, October 2002, pp. 187–192.
[23] J. B. Bryan, Precis. Eng. **1**, 129 (1979).
[24] N. Troisfontaine, P. Bidaud, and M. Larnicol, Smart Mater. Struct. **8**, 197 (1999).